Global view of refilling of the plasmasphere

Bill R. Sandel[1] and Michael H. Denton[2,3]

Received 11 May 2007; revised 24 June 2007; accepted 8 August 2007; published 7 September 2007.

[1] We use observations by the IMAGE Extreme Ultraviolet Imager (EUV) to characterize the outflow of He^+ from the ionosphere to the plasmasphere under quiet conditions. The view afforded by the IMAGE orbit encompasses the entire plasmasphere in a single exposure, enabling us to examine for the first time the globally-averaged properties of plasmasphere refilling. We focus on a study period that begins with a moderate erosion event, and follow refilling during multiple orbits for a period of 69 hours. The inferred volume refilling rate, averaged over azimuth and time, ranges from $\sim$1 He^+ cm^{-3} h^{-1} at $L = 3.3$ to $\sim 7 \times 10^{-2}$ He^+ cm^{-3} h^{-1} at $L = 6.3$ and is generally consistent with earlier, more local measurements. We show that the measured radial abundance profiles match those predicted by the Sheffield University Plasmasphere Ionosphere Model (SUPIM) for $2 \leq L \leq 4$. **Citation:** Sandel, B. R., and M. H. Denton (2007), Global view of refilling of the plasmasphere, *Geophys. Res. Lett.*, *34*, L17102, doi:10.1029/2007GL030669.

1. Introduction

[2] The plasmasphere is a region of cold (<1 eV) and relatively dense plasma in the inner magnetosphere. It extends from Earth's upper atmosphere (and is in some senses an extension of the atmosphere) to an outer boundary called the plasmapause. The plasmasphere is populated by ions and electrons in dynamic equilibrium with the upper ionosphere. The principal positive ions are H^+ and He^+, very roughly in the ratio of 10:1, with a variable component of O^+. This plasma does not experience magnetic gradient and curvature drifts because of its low energy, but rather corotates (approximately) with Earth, often lagging behind corotation by 10–15% in angular velocity [*Sandel et al.*, 2003].

[3] The location of the plasmapause varies with magnetic activity. During quiet periods, the plasmasphere expands past $L = 7$ toward a "saturated" configuration. During active times, enhanced magnetospheric convection leads to erosion of the outer regions of the plasmasphere, and the plasmapause moves inward to $L \sim 3$, and occasionally to $L \sim 2$. Thus the plasmasphere is constantly in a state of change, contracting in a few hours in response to increasing activity and refilling over a period of a few days in quiet times [e.g., *Kersley and Klobuchar*, 1980].

[4] Both processes have received much experimental and theoretical attention [e.g., *Lemaire and Gringauz*, 1998]. Recently, global imaging has played an important role in the study of one of these processes, namely erosion [e.g., *Goldstein et al.*, 2003, 2005]. However, the advantages of global plasmasphere imaging have not yet been fully exploited in studies of the physics of plasmasphere refilling, and that is our focus here. These global measurements augment and complement recent, more localized measurements using in situ techniques [e.g., *Su et al.*, 2001; *Carpenter et al.*, 1993], and ground-based magnetometers [e.g., *Chi et al.*, 2000; *Dent et al.*, 2006].

[5] Here we study refilling of the plasmasphere after an erosion event. We compare radial profiles and refilling rates determined from the Extreme Ultraviolet Imager (EUV) on the IMAGE Mission with results from the Sheffield University Plasmasphere Ionosphere Model (SUPIM). We adjust the initial conditions of the model to match the eroded plasmasphere, and then compare modeled and measured refilling. From the measured column abundances, we infer volume refilling rates near the plane of the magnetic equator, and compare with earlier measurements and models.

2. Observations

[6] We use observations of the plasmasphere by EUV [*Sandel et al.*, 2000, 2003] during the interval 27–30 June 2001. EUV maps the distribution of He^+ in the plasmasphere by imaging light scattered by He^+ at its resonance wavelength of 30.4 nm. Because the plasmasphere is optically thin at this wavelength, the recorded brightness is proportional to the column abundance of He^+ integrated along the lines of sight corresponding to each pixel. The time resolution of each image is about 10 min and the spatial resolution is 0.6°, or about 0.1 R_E in the plane of the magnetic equator seen from apogee.

[7] The best time to study plasmasphere refilling is during an extremely quiet period following a moderate erosion event. Then there would be no confounding effects such as episodes of weak convection, which could decrease apparent refilling rates. We could confidently ascribe any changes in plasma abundances to upward flow from the ionosphere. Such ideal conditions occur infrequently. The time period during the IMAGE Mission that best fulfills these criteria, and offers good coverage by EUV, is 27–30 June 2001 (2001/178 to 181) and we focus on this period here. At this time, the apogee of the IMAGE satellite was at high northern latitudes, affording excellent views of the entire plasmasphere. This viewing geometry has already been used to advantage in previous investigations of this event using IMAGE data [*Denton et al.*, 2007].

[8] The line plots in Figure 1 show the magnetic conditions. Prior to $t = 0$ h, the Z-component of the solar wind magnetic field was predominantly southward; we expect

[1]Lunar and Planetary Laboratory, University of Arizona, Tucson, Arizona, USA.
[2]Department of Communication Systems, Lancaster University, Lancaster, UK.
[3]Previously at ISR-1, Los Alamos National Laboratory, Los Alamos, New Mexico, USA.

0094-8276/07/2007GL030669$05.00

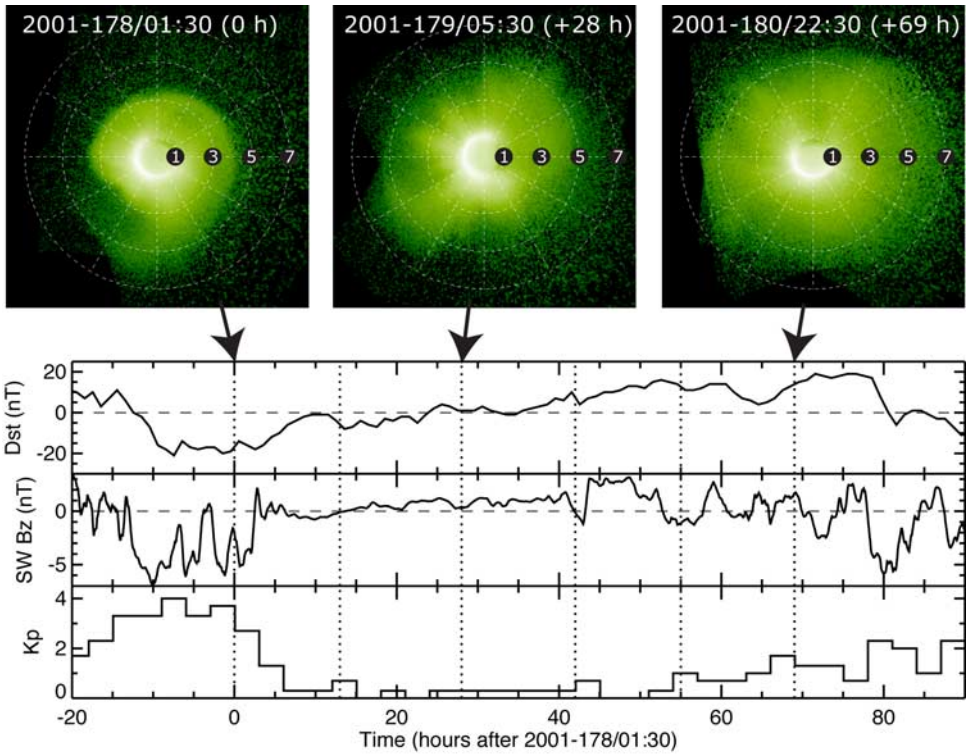

Figure 1. (top) Brightness of the 30.4-nm resonance line of He^+ in the plasmasphere for the early, middle and late parts of the period used for the refilling study. (bottom) Geomagnetic conditions and solar wind B_z in the GSE system (from ACE/MAG) before, during, and after the study period. The vertical dotted lines mark the times of the six images used here.

convection to erode the plasmasphere, moving the plasmapause inward [*Goldstein et al.*, 2003]. A long period of quiet began a few hours after $t = 0$ h. Until $t \sim 70$ h, B_z was positive (or slightly negative for short intervals), $K_P \leq 2$, and Dst was near zero or positive. Because for these quiet conditions the plasmapause is expected to lie near or outside $L = 6$ [*O'Brien and Moldwin*, 2003], loss of plasmaspheric material by convection should be minimal, so that we can ascribe the net observed changes in ion abundance to refilling from the ionosphere.

[9] We select several EUV frames from near apogee in each of six consecutive IMAGE orbits, spanning the time $t = 0$–69 h. For each orbit set, we project the frames to the plane of the magnetic equator [*Sandel et al.*, 2003] and sum them. We use two sets of projections, one with magnetic longitude as the azimuthal coordinate (Set A) and one with magnetic local time (Set B). Figure 1 shows three of the resulting six images from Set A, used for this illustration because nearly corotating features are smeared less by the extended integration time. As expected, convection eroded the plasmasphere so that at $t = 0$ h the plasmapause is sharply defined near $L \sim 3$–4. At 28 h, the plasmasphere has expanded, its interior is structured in azimuth, and the plasmapause is diffuse. Finally, at 69 h the plasmapause lies outside $L = 6$ and the interior is less structured in azimuth.

[10] To focus on the global-scale behavior of the plasmasphere, we bin each of the six images in Set B in steps of 0.5 R_E in radius, summing over all local times, but excluding Earth's shadow. Converting the measured He^+ 30.4-nm brightness to He^+ column abundance using the method described by *Gallagher et al.* [2005] gives the azimuthally-averaged radial profiles of column abundance in Figure 2. The number of pixels in the annular bins ranges from ~700 at $L = 2.25$ to ~1900 at $L = 6.25$. The summations for each orbit include 5 to 8 images, with the average value being 5.8. Owing to the many pixels in each spatial bin and the summation of several 10-min images, the statistical uncertainties in the points are smaller than the

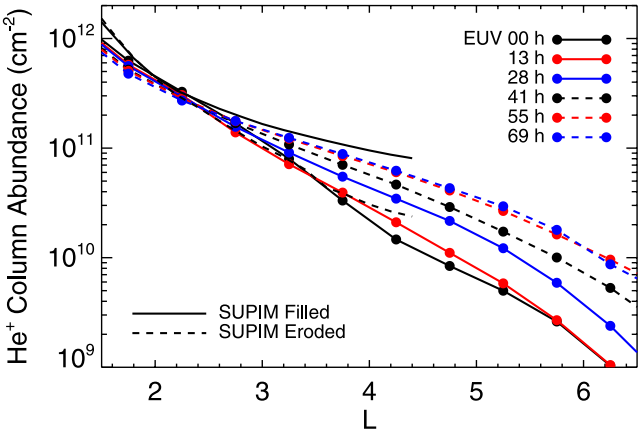

Figure 2. Radial profiles of He^+ column abundance for six times during the refilling study. The abundance profiles increase steadily with increasing time, reflecting refilling of the plasmasphere. The black lines without points show column abundances calculated from SUPIM for the same observing geometry.

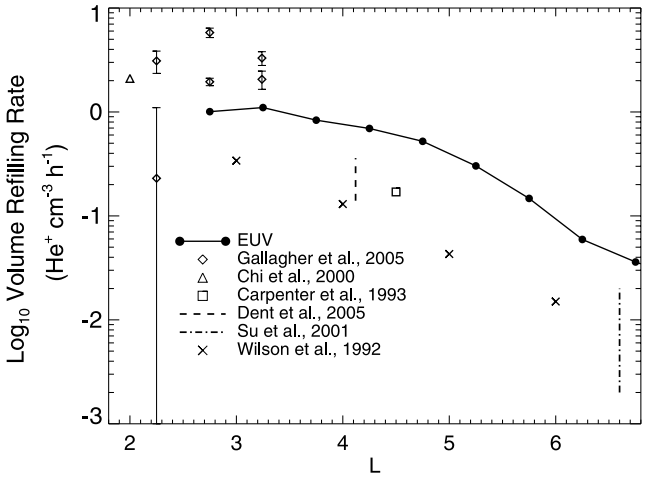

Figure 3. Volume refilling rates at the equator for He^+. The EUV curve shows the refilling rate for our study period, and the symbols show other measurements and models. For most of the measurements, we have estimated the He^+ rate from other measured quantities. The vertical lines for the *Su et al.* [2001] and *Dent et al.* [2006] measurements represent the range of reported values.

plotted symbols. Based on our ground photometric calibration, updated in flight by observations of the Moon, we estimate that systematic errors arising from the uncertainty in calibration are about 20%.

[11] The profiles in Figure 2 show that, for this study period, the effects of erosion and refilling were confined to regions for which $L \geq 3$. The refilling progression is quite orderly and smooth, with higher column abundances at each succeeding time-step for almost all values of L within the affected region. The step between 0 h and 13 h is smaller than for the later intervals. The history of B_z in Figure 1 suggests a cause: the period of erosion extended a few hours past $t = 0$ h, so that the time devoted to refilling between images from the first pair of orbits was atypically small, compared to later pairs. This behavior is also qualitatively consistent with a lower early-time refilling rate [*Su et al.*, 2001]. Because of the uncertainties in the initial conditions and the limited time resolution of our analysis, it is difficult to quantify this in detail.

3. Comparing With SUPIM

[12] The Sheffield University Plasmasphere Ionosphere Model (SUPIM) solves coupled time-dependent equations of continuity, momentum and energy balance along closed magnetic field lines for six ion species (O^+, H^+, He^+, N_2^+, O_2^+ and NO^+) and the electrons [*Bailey et al.*, 1997]. Inputs include the solar EUV flux from the EUVAC model [*Richards et al.*, 1994], the MSIS 86 neutral atmosphere model [*Hedin*, 1987], and the HWM90 model of meridional and zonal wind velocities [*Hedin et al.*, 1991]. Outputs include the ion and electron densities, temperatures, and field-aligned fluxes. In the current model we calculate the He^+ (and electron) densities along 159 individual flux tubes in the range $1 < L < 13.5$ to generate 2D meridional slices through the plasmasphere/ionosphere system at fixed longitudes.

[13] To compare the model results with the measured profiles, we first compute column abundances for the model using realistic observing geometry, and then average over azimuths in a way similar to that used for the EUV images. We began the model comparison by adjusting the initial conditions of the model to match the column abundances measured for the eroded plasmasphere at $t = 0$. This was achieved by increasing the neutral helium density in the MSIS 86 neutral atmosphere used as input to the model sixfold. We also experimented with increasing the He^+ density by increasing equatorial $\mathbf{E} \times \mathbf{B}$ drifts, but this was less effective. Owing to the relative inertness of He and He^+, increasing their abundance does not lead to large changes in the ionospheric chemistry.

[14] The lower of the SUPIM curves ("Eroded") in Figure 2 shows good agreement with the $t = 0$ h profile. From this starting plasma distribution, the model predicts the radial profiles of column abundances at later times. The upper SUPIM curve ("Filled") in Figure 2 shows the model profile corresponding to that measured by EUV at $t = 69$ h. The excellent agreement between the SUPIM curve and the measured profile for $t = 69$ h shows that the model has done a good job of correctly predicting refilling rates for this time interval over the range $2 \leq L \leq 4$. Beyond $L \approx 4$, SUPIM densities diverge increasingly from the EUV observations, and in fact there appears to be a point of inflection in the curves shown in Figure 2. This difference between model and data is probably a signature of physical processes not accounted for in SUPIM in the region beyond $L \approx 4$, an area that is currently under investigation.

4. Volume Refilling Rates

[15] In the previous section we used information from SUPIM on the distribution of He^+ along the field lines to compute model column abundances and then compared these directly with the EUV measurements. However, most previous measurements of plasmasphere refilling have been interpreted to yield the volume rate of refilling near the magnetic equator, and that is also the quantity computed by most models. In this section we use the time derivative of the EUV column abundances to estimate the volume refilling rate near the equator, so that we can compare EUV measurements with these earlier measurements and models.

[16] The time derivative of the column density is easy to compute from the curves in Figure 2. We convert these results to volume rates at the equator using the concept of effective pathlength along EUV lines of sight [*Gallagher et al.*, 2005]. Since SUPIM provides a good fit to the radial profiles, we estimate the radially-varying effective pathlength by comparing model volume abundances with the column abundances computed from the same model. Typical values of the effective pathlength range from $\sim$1.7 R_E at $L = 2$ to $\sim$2.3 R_E at $L = 6$. The EUV plot in Figure 3 shows the volume refilling rate at the equator determined in this way, and averaged over the full 69-h study interval. The statistical uncertainties propagated from the curves in Figure 2 are again smaller than the plotting symbols. However, computing volume rates from column abundances using the effective path length introduces an additional

source of error. We estimate that the combined systematic errors do not exceed 50% [*Gallagher et al.*, 2005].

[17] Figure 3 also shows the He^+ refilling rates inferred by *Gallagher et al.* [2005] for a special circumstance: the target area was a notch in the plasmasphere, observed when geomagnetic activity was more complex than in our study period. The two groups of three points (at L = 2.25, 2.75, and 3.25) represent refilling inferred from two pairs of orbits, and in the intervening pair, *Gallagher et al.* [2005] observed depletion. In spite of the special circumstances, these points fit fairly well with the general trend from our new measurements, which are based on a more comprehensive data set.

[18] To compare He^+ refilling rates inferred from EUV with other measurements and models, we must account for the fact that the quantities reported from the measurements and models usually do not include the He^+ abundance specifically. For example, to convert rates based on measurements of electron or ion density [e.g., *Carpenter et al.*, 1993; *Su et al.*, 2001], we have used an estimate of the ratio $\alpha = n(He^+)/n(H^+)$ from the parameterization described by *Craven et al.* [1997]. The value of α ranged from 0.094 at L = 2 to 0.018 at L = 6.6. Further, we have used the approximation that H^+ and He^+ are the only positive ions, but in fact some heavier ions, particularly O^+, are present.

[19] The measurements of *Su et al.* [2001] encompass a wide span of times and conditions at geosynchronous orbit, but here we simply represent the full range of their determinations by a vertical bar. For consistency, we use the parameterization of α to infer a He^+ refilling rate, even though the measurements used by *Craven et al.* [1997] to define α extend to a distance of only 4.7 R_E. The value of α decreases at a rate of $\sim$50% R_E^{-1}. If our extrapolation underestimates α at 6.6 R_E, then the He^+ refilling rate that we infer from the Su et al. measurements should be increased, and would then agree better with EUV measurements.

[20] Inferring the He^+ refilling rate from the mass density measurements [e.g., *Chi et al.*, 2000; *Dent et al.*, 2006] in this way carries more uncertainty because heavier ions contribute proportionally more to the mass density than to the charge density. Since we have neglected the contribution of heavier ions, in particular O^+, it is likely that we have over-estimated the He^+ refilling rate from the mass density measurements. Assuming a 3% fraction of O^+ reduces the inferred He^+ rate by $\sim$30%. Nevertheless, the measurement of *Chi et al.* [2000] is consistent with a value obtained by extrapolating the EUV curve to lower L.

[21] The measurements of *Chi et al.* [2000], *Dent et al.* [2006], and *Carpenter et al.* [1993] refer to specific locations and times, and hence to particular geomagnetic conditions, which differ from those during our study interval. The Dent et al. measurements come from a more active time (K_P = 2 to 4, with some B_z excursions to -5 nT). For the Carpenter et al. measurements, K_P varied from 2^+ to 1, and the Chi et al. measurements followed a large storm.

[22] For the refilling rates credited to the model of *Wilson et al.* [1992], we used the data on H^+ densities in their Figure 9 and averaged over 48 h, the longest time for which information was available from the figure. Because the abundance profiles measured by EUV changed only slightly between the samples at t = 55 and 69 h, the EUV and models results should be approximately comparable. Nevertheless the model falls substantially below EUV measurements, and departs more at larger L. The departure at larger L may reflect our use of an inappropriate extrapolation of α as described above.

5. Discussion

[23] The curves in Figure 2 indicate that refilling had asymptotically slowed by an elapsed time of 69 h. Some work has found a longer time to this condition of "saturation" [e.g., *Kersley and Klobuchar*, 1980; *Carpenter et al.*, 1993]. But we remember that our measurements refer to the He^+ refilling rate, which is usually not the quantity measured or modeled in earlier work. It is possible that interspecies differences in refilling rates contribute to the differences mentioned above. We plan additional work to investigate this possibility by comparing He^+ abundances measured by EUV with electron abundances from IMAGE/RPI, and continued work with SUPIM.

[24] The supply of plasma from the ionosphere to the plasmasphere is a fundamental aspect of ionosphere-magnetosphere coupling. Owing to its global view, IMAGE EUV can measure many radial profiles of He^+ column abundance simultaneously. No other technique gives information on many positions in L and local time simultaneously. Furthermore, using EUV observations, we can avoid interpreting changes in abundance driven by sub-corotation as purely temporal changes, an error to which in situ and ground-based techniques may be subject. We plan to exploit this by further investigations of such questions as early vs. late refilling rates, the dependence on magnetic and solar activity, and possible longitude dependencies.

[25] **Acknowledgments.** We acknowledge Graham Bailey's efforts in developing SUPIM. MD thanks Graham Bailey and Michelle Thomsen (LANL) for many helpful discussions. Work at the University of Arizona was funded by a subcontract from Southwest Research Institute under NASA contract NAS5-96020 with SwRI, and by NASA grant NNX07AG46G. We thank the ACE SWEPAM and MAG instrument teams and the ACE Science Center for providing the ACE data. We thank the reviewers for helpful comments.

References

Bailey, G. J., N. Balan, and Y. Z. Su (1997), The Sheffield University plasmasphere ionosphere model—A review, *J. Atmos. Terr. Phys.*, *59*, 1541–1552.

Carpenter, D. L., B. L. Giles, C. R. Chappell, P. M. E. Décréau, R. R. Anderson, A. M. Persoon, A. J. Smith, Y. Corcuff, and P. Canu (1993), Plasmasphere dynamics in the duskside bulge region: A new look at an old topic, *J. Geophys. Res.*, *98*, 19,243–19,272.

Chi, P. J., C. T. Russell, S. Musman, W. K. Peterson, G. Le, V. Angelopoulos, G. D. Reeves, M. B. Moldwin, and F. K. Chun (2000), Plasmaspheric depletion and refilling associated with the September 25, 1998 magnetic storm observed by ground magnetometers at L = 2, *Geophys. Res. Lett.*, *27*, 633–636.

Craven, P. D., D. L. Gallagher, and R. H. Comfort (1997), Relative concentration of He^+ in the inner magnetosphere as observed by the DE 1 retarding ion mass spectrometer, *J. Geophys. Res.*, *102*, 2279–2290.

Dent, Z. C., I. R. Mann, J. Goldstein, F. W. Menk, and L. G. Ozeke (2006), Plasmaspheric depletion, refilling, and plasmapause dynamics: A coordinated ground-based and IMAGE satellite study, *J. Geophys. Res.*, *111*, A03205, doi:10.1029/2005JA011046.

Denton, M. H., M. F. Thomsen, B. Lavraud, M. G. Henderson, R. M. Skoug, H. O. Funsten, J.-M. Jahn, C. J. Pollock, and J. M. Weygand (2007), Transport of plasma sheet material to the inner magnetosphere, *Geophys. Res. Lett.*, *34*, L04105, doi:10.1029/2006GL027886.

Gallagher, D. L., M. L. Adrian, and M. W. Liemohn (2005), Origin and evolution of deep plasmaspheric notches, *J. Geophys. Res.*, *110*, A09201, doi:10.1029/2004JA010906.

Goldstein, J., B. R. Sandel, W. T. Forrester, and P. H. Reiff (2003), IMF-driven plasmasphere erosion of 10 July 2000, *Geophys. Res. Lett.*, *30*(3), 1146, doi:10.1029/2002GL016478.

Goldstein, J., J. L. Burch, and B. R. Sandel (2005), Magnetospheric model of subauroral polarization stream, *J. Geophys. Res.*, *110*, A09222, doi:10.1029/2005JA011135.

Hedin, A. E. (1987), MSIS-86 thermospheric model, *J. Geophys. Res.*, *92*, 4649–4662.

Hedin, A. E., N. W. Spencer, M. A. Biondi, R. G. Burnside, G. Hernandez, and R. M. Johnson (1991), Revised global model of thermosphere winds using satellite and ground-based observations, *J. Geophys. Res.*, *96*, 7657–7688.

Kersley, L., and J. A. Klobuchar (1980), Storm associated protonospheric depletion and recovery, *Planet. Space Sci.*, *28*, 453–458, doi:10.1016/0032-0633(80)90026-4.

Lemaire, J. F., and K. I. Gringauz (1998), *The Earth's Plasmasphere*, Cambridge Univ. Press, New York.

O'Brien, T. P., and M. B. Moldwin (2003), Empirical plasmapause models from magnetic indices, *Geophys. Res. Lett.*, *30*(4), 1152, doi:10.1029/2002GL016007.

Richards, P. G., J. A. Fennelly, and D. G. Torr (1994), EUVAC: A solar EUV flux model for aeronomic calculations, *J. Geophys. Res.*, *99*, 8981–8992.

Sandel, B. R., et al. (2000), The Extreme Ultraviolet Imager investigation for the IMAGE mission, *Space Sci. Rev.*, *91*, 197–242.

Sandel, B. R., J. Goldstein, D. L. Gallagher, and M. Spasojević (2003), Extreme Ultraviolet Imager observations of the structure and dynamics of the plasmasphere, *Space Sci. Rev.*, *109*, 25–46, doi:10.1023/B:SPAC.0000007511.47727.5b.

Su, Y.-J., M. F. Thomsen, J. E. Borovsky, and D. J. Lawrence (2001), A comprehensive survey of plasmasphere refilling at geosynchronous orbit, *J. Geophys. Res.*, *106*, 25,615–25,630.

Wilson, G. R., J. L. Horwitz, and J. Lin (1992), A semikinetic model for early stage plasmasphere refilling: 1. Effects of coulomb collisions, *J. Geophys. Res.*, *97*, 1109–1119.

M. H. Denton, Space Plasma Environment and Radio Science, Department of Communication Systems, Lancaster University, Lancaster LA1 4WA, UK.

B. R. Sandel, Lunar and Planetary Laboratory, University of Arizona, 1541 E. University Boulevard, Tucson, AZ 85721, USA. (sandel@arizona.edu)